00-30130 [7]
Translated from Russian

UDC 539.171.017

EVALUATION OF ANGULAR DISTRIBUTIONS AND PRODUCTION CROSS-SECTIONS FOR DISCRETE GAMMA LINES IN IRON

M.V. Savin, A.V. Livke, A.G. Zvenigorodskij
Russian Federal Nuclear Centre - All-Russia Scientific Research Institute for Experimental Physics, Sarov

EVALUATION OF ANGULAR DISTRIBUTIONS AND PRODUCTION CROSS-SECTIONS FOR DISCRETE GAMMA-LINES IN IRON. The experimental data were compiled and the angular distributions and production cross-sections for the E_γ = 846.8, 1238.3 and 1810.8 keV discrete gamma-lines evaluated. The Legendre polynomial coefficients describing the angular distributions in the energy range up to E_n = 14.0 MeV and cross-section values in the E_n = 0.85-19.0 MeV range were evaluated.

Discrete gamma line production cross-sections are of interest because they can be used in a number of practical applications as basic information on the phenomena under investigation. In addition, discrete gamma lines can be used as reference (standard) cross-sections when carrying out measurements and evaluations.

In this paper, we have compiled the experimental data and evaluated the angular distributions and production cross-sections for the following main gamma lines of ^{56}Fe: E_γ = 846.8 keV (transition from the first level E_{lev} = 846.8(2^+) to the ground state (0^+)); E_γ = 1238.3 keV (transition from the second level E_{lev} = 2085.1 keV (4^+) to the first level); and E_γ = 1810.8 keV (transition from the third level E_{lev} = 2657.6 keV (2^+) to the first level).

A statistical approximation of the data files was produced using splines. With adequate data, the spline approximation program developed by V.A. Zherebtsov [1] produces reliable averaged curves automatically selecting the spline knots. Furthermore, the possibility is provided of intervening in the evaluator's approximation process, changing the weighting of certain data and/or selecting additional knots and boundary conditions in order to improve the statistical description of the data files.

The spline approximation results are presented in the form of tables of knot values and spline polynomial coefficients from which the value of the function Si(h) can be calculated at any point using the following expression:

$$S_i(h) = A_o + A_1 h + A_n h^n, \quad (1)$$

where $h = X - X_i$, X_i being the left boundary (knot) of the corresponding interval.

In the experiments, the discrete gamma line production cross-sections were measured at different angles to the neutron beam axis by the various authors. It would therefore be wrong to make a direct comparison of results, particularly in the neutron energy region close to the gamma production excitation energy in the nucleus. Therefore, the angular distributions of the discrete gamma rays were first of all evaluated.

1. Angular distributions

The angular distributions of discrete gamma rays $\sigma(\theta)$ produced by inelastic interaction of neutrons are described with adequate accuracy by the even terms of the Legendre polynomial. In most cases, a good description of the angular distributions can be achieved using only three terms: P_0, P_2 and P_4.

$$\sigma(\theta)=\frac{\sigma_0}{4\pi}(1+\alpha_2 P_2(\theta)+\alpha_4 P_4(\theta)) \qquad (2)$$

In the evaluation process, the coefficients α_2 and α_4 (2) were found using the method of least squares and all the available experimental data [2-6] on angular distributions for the main 847, 1240 and 1810 keV gamma lines. The results obtained are given in Tables 1-3. These tables also give references to sources whose results were used to obtain the coefficients α_2 and α_4. In a number of cases, values for α_2 and α_4 given by the authors of experimental papers were used. The values of the coefficients are given in Figs 1-3.

The figures show that very few experimental data are available for reliable determination of the energy dependences of the expansion coefficient $\alpha_{2,4}(E_n)$, and the available results show a poor level of integral agreement. We therefore used calculated results for the angular distributions produced using the Hauser-Feshbach statistical model of the nucleus, taking into account competition from electromagnetic transitions in cascade decay of excited states [7]. These results are also given in Tables 1-3 and in the figures.

As the figures show, any form of statistical approximation of the data is unlikely to yield sensible results. Therefore, first of all, we performed a spline approximation of the energy dependences $\alpha_2(E_n)$ and $\alpha_4(E_n)$ selecting spline knots and changing the weightings of experimental data. The results obtained were then corrected slightly to take account of the general pattern of the dependence of the angular distributions on the extent to which the neutron energy exceeds the energy of the level from which gamma rays are emitted.

The values of the α_4 coefficients for the E_γ = 1240 and 1810 keV gamma lines have a wide spread. Since the α_4 coefficients for these gamma lines are low, we assumed $\alpha_4 = 0$ for these gamma lines. The error in the description of angular distributions for this kind of approximation relative to the ratio of the coefficients α_2 and α_4 may be 0.5-2%.

The evaluated values of the coefficients α_2 and α_4 are shown in Figs 1-3 as a continuous line.

Table 1

Experimental and calculated values of the coefficients in the expansion of the angular distributions using the Legendre polynomial for the E_γ = 846.8 keV gamma line

Experimental data								Calculated data [7]		
E_n (MeV)	α_2	α_4	Ref.	E_n (MeV)	α_2	α_4	Ref.	E_n (MeV)	α_2	α_4
0.95	0.464	-0.484	[5]	0.98	0.5395	-0.303	[4]	2.8	0.172	-0.0449
1.05	0.504	-0.247	[5]	1.08	0.4355	-0.142	[4]	3.1	0.174	-0.0432
1.5	0.223	-0.169	[5]	1.18	0.3996	-0.3323	[4]	3.5	0.175	-0.0473
2.5	0.178	-0.050	[3]	1.28	0.305	0	[4]	4	0.169	-0.0549
2.8	0.3335	0.117	[6]	1.38	0.3852	0	[4]	6	0.129	-0.0701
3.1	0.152	-0.077	[5]	1.59	0.323	-0.1531	[4]	7.5	0.115	-0.0656
3.5	0.193	-0.005	[5]	1.68	0.2226	-0.1547	[4]	7.95	0.112	-0.0632
4	0.149	-0.033	[5]	1.79	0.2167	-0.0840	[4]	8.5	0.108	-0.0004
6	0.231	0.024	[2]	1.85	0.2409	-0.0974	[4]	9	0.104	-0.058
7.5	0.19	-0.084	[2]	2.03	0.1842	-0.0238	[4]	14.1	0.0756	-0.0384
8.8	0.1887	0.028	[3]							
14.1	0.09	-0.1	[3]							

Table 2

Experimental and calculated values of the coefficients in the expansion of the angular distributions using the Legendre polynomial for the E_γ = 1238.3 keV gamma line

Experimental data				Calculated data [7]		
E_n (MeV)	α_2	α_4	Ref.	E_n (MeV)	α_2	α_4
2.5	0.302	0.0239	[3]	2.8	0.34	-0.0772
2.8	0.635	0.0146	[6]	3.1	0.341	-0.0781
3.1	0.243	0.0627	[5]	3.5	0.34	-0.0798
3.5	0.387	-0.0705	[5]	4	0.337	-0.0829
4	0.289	-0.0514	[5]	6	0.268	-0.0537
6	0.263	-0.0103	[2]	7.5	0.228	-0.0319
7.5	0.633	0.127	[2]	7.95	0.219	-0.028
8.8	0.22	-0.045	[3]	8.5	0.21	-0.0246
14.1	0.14	-0.1	[3]	9	0.203	-0.0225
				14.1	0.157	-0.0179

Table 3

Experimental and calculated values of the coefficients in the expansion of the angular distributions using the Legendre polynomial for the E_γ = 1810.8 keV gamma line

Experimental data				Calculated data [7]		
E_n (MeV)	α_2	α_4	Ref.	E_n (MeV)	α_2	α_4
2.8	0.491	0.29	[6]	2.8	0.444	-0.00214
3.1	0.236	0.0604	[5]	3.1	0.405	-0.00188
3.5	0.273	0.067	[5]	3.5	0.301	-0.00129
4	0.1075	-0.0146	[5]	4	0.245	-0.00081
6	-0.0003	0.027	[2]	6	0.194	-0.00061
7.5	0.0026	-0.1235	[2]	7.5	0.158	-0.00063
8.8	0.067	0.021	[3]	7.95	0.15	-0.00061
				8.5	0.142	-0.00058
				9	0.135	-0.00056
				14.1	0.092	-0.00036

2. Discrete gamma-ray production cross-sections

A large number of measurements were made at the early stage of research, mostly using gamma-ray scintillation spectrometers. However attractive these spectrometers may be, their energy resolution is insufficient for a detailed study of the line structure of spectra. A set of closely grouped gamma lines is registered by these detectors as one line, which introduces an uncertainty into the discrete line production cross-section being measured. Therefore, in the main, we only looked at data obtained using detectors with a high energy resolution. Moreover, we did not use results obtained via relative measurements (mainly for the E_γ = 847 keV gamma line in iron). The whole set of studies may be divided into three groups: studies carried out using 14-15 MeV (d,T) neutrons [2, 8-14]; measurements performed using monochromatic neutrons over a wide energy range [15-18]; and studies carried out for a continuous spectrum using the time-of-flight method [19-23].

A few comments on some of the experiments.- In Ref. [8], the measurement results were normalized to the production cross-section value for the E_γ = 4.43 MeV gamma line in carbon at a neutron energy of E_n = 14.8 MeV. The iron sample, which was a disk 15 cm in diameter and about 3 cm thick, was positioned 10 cm from the neutron source. The measurement geometry, sample dimensions and data normalization are not optimal. The measurement error given by the authors of 1%, 3% and 10% for the 847, 1240 and 1810 keV lines respectively is improbable. In Ref. [13], the authors do not indicate the error for determination of the distance between the neutron source and the sample, which could be considerable in the "compact" geometry used for the measurements. In Ref. [14], the time-of-flight method is used to separate out neutrons and gamma rays from the sample. However, since the distance between the detector and the sample was 30 cm and the time resolution 7.5 ns, as the paper indicates, it is doubtful the separation would be adequate and that there would not be additional uncertainty in the cross-section value.

Although Refs [20, 21] used an NaI(Tl) detector, we did take the results of this study for the E_γ = 846.8 keV gamma line into consideration, because the work was carried out sufficiently correctly for a wide neutron energy range and the contribution of adjacent gamma lines to the 847 keV gamma line peak (787.8 and 869 keV lines at $E_n > 3.5$ MeV) is negligible.

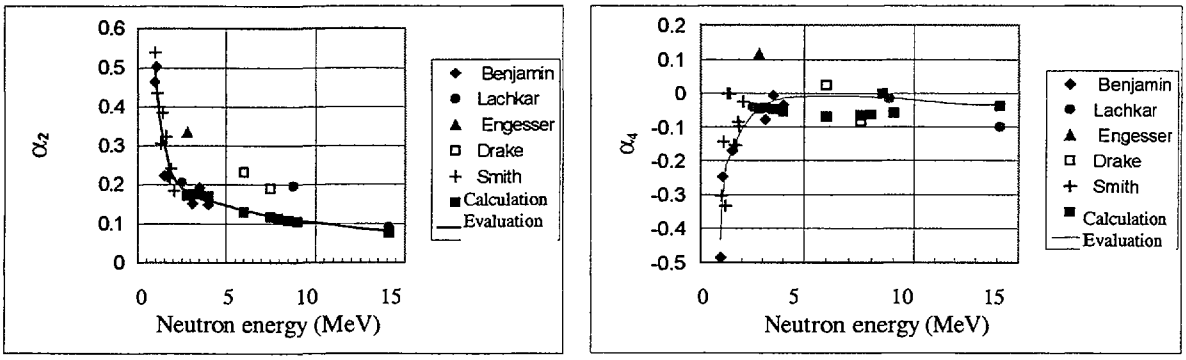

Fig. 1. Values of the coefficients α_2 and α_4 of the Legendre polynomials used to describe the angular distributions of the E_γ = 846.8 keV gamma line.

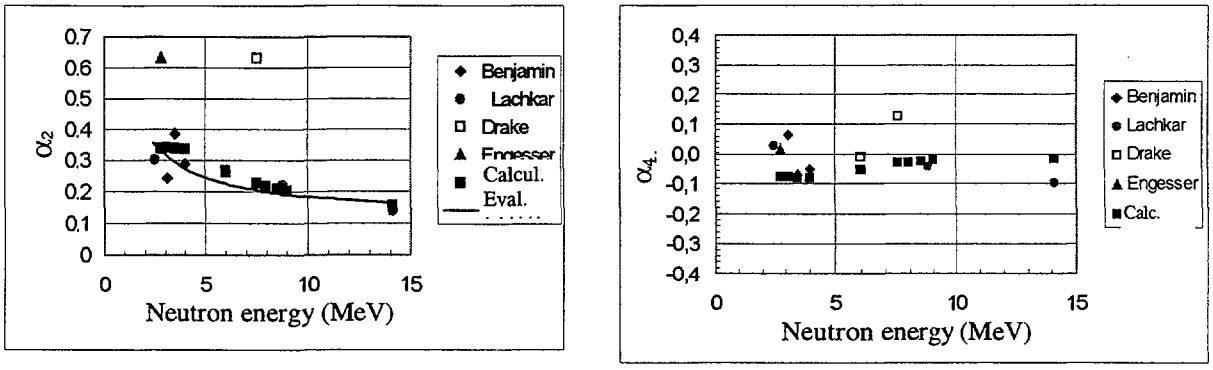

Fig. 2. Values of the coefficients α_2 and α_4 of the Legendre polynomials used to describe the angular distributions of the E_γ = 1238.3 keV gamma line.

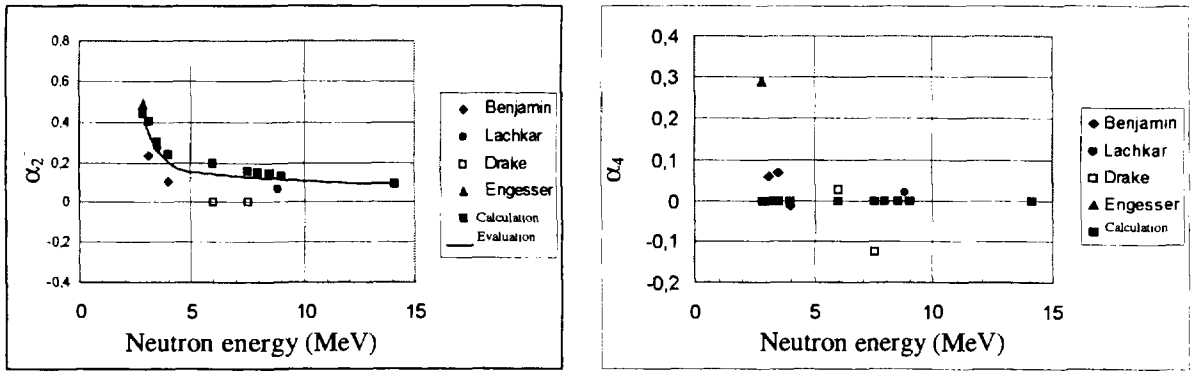

Fig. 3. Values of the coefficients α_2 and α_4 of the Legendre polynomials used to describe the angular distributions of the E_γ = 1810.8 keV gamma line.

As mentioned earlier, in the various studies the gamma-ray detectors were positioned at different angles when measuring the discrete gamma line production cross-sections. Furthermore, some authors give data for ^{56}Fe and others for the natural isotopic composition, even though the 847, 1240 and 1810 lines are formed as a result of excitation and decay of the ^{56}Fe nucleus. With a view to presenting the results of different authors on the same scale, all the available experimental data were normalized to the natural isotope mixture (^{56}Fe content - 0.91754) and reduced to the angle-integrated production cross-section σ_0 for the specific gamma line using the formula

$$\sigma_0 = \frac{4\pi\sigma(\theta)}{1+\alpha_2 P_2(\theta)+\alpha_4 P_4(\theta)}, \qquad (3)$$

where θ is the angle at which the differential cross-section was measured.

In formula (2), the Legendre polynomial coefficients α_2 and α_4 from our evaluation were used.

Where the data were obtained using a continuous spectrum neutron source and the time-of-flight method, the average neutron energy for each interval ΔE_n was determined on the basis that, in the experiment, events are registered at evenly distributed intervals of times of flight Δt. Here, the average energy corresponding to the average interval time will be:

$$E_{avi} = \frac{4}{\left(\frac{1}{\sqrt{E_{1i}}}+\frac{1}{\sqrt{E_{2i}}}\right)^2}, \qquad (4)$$

where E_{1i} and E_{2i} are the lower and upper limits of the ith interval given in the tabulated data. For low neutron energies, determining the average interval energy in this way yields a result which hardly differs from the simple average: $E_{av} = (E_1 + E_2)/2$. At high energies, the difference becomes significant, which is particularly important in the $E_n \geq 10$ MeV region where there is a sharp dip in the cross-sections owing to decay channel competition.

846.8 keV gamma line

The experimental values for the angle-integrated 846.8 keV gamma line production cross-sections are shown in Figs 4-5. In order not to clutter the diagrams, the measurement errors are not shown, since they differ but little in the various studies, lying in the 10-15% range. All measurement errors were taken into account when performing the approximation of the data.

The experimental results of the different authors show a fair level of agreement in the main, apart from some of Drake's values [2] which are noticeably higher than the overall data. The considerable spread of the data obtained using 14-16 MeV monoenergetic neutrons is somewhat surprising; here, one could expect a better level of agreement. This broad spread may be due to the fact that these measurements were performed in a "compact" geometry, resulting in a high level of uncertainty in the magnitude of the neutron flux onto the sample.

Near the excitation threshold of the level ($E_{thr} \leq E_n \leq 3$ MeV), the energy dependence of the production cross-section for the 846.8 keV line, resulting from a dipole ($2^+ \rightarrow 0^+$) transition, has a complex structure. This structure is delineated particularly well in Ref. [22] by Voss. Voss's data, which are averaged over the $\Delta E_n \cong 50$ keV interval are shown in Figs 4-5 as a continuous line.

In the $E_n < 3$ MeV neutron energy region, to obtain an "averaged" curve when performing the spline approximation a higher number of spline knots was specified. In the $E_n \geq$ 2.8 MeV neutron energy region where the structure may be ignored, only two knots were specified. The overall evaluated cross-section curve for the 846.8 keV line is shown in Figs 4-5 as a continuous line.

1238.3 keV line

The experimental data and the results of the evaluation for the 1238.3 keV gamma line production cross-section are shown in Fig. 6. Voss's results [22] were averaged over broad energy intervals - at the beginning of the scale $\Delta E = 0.2$ MeV, and subsequently $\Delta E \cong 0.5$ MeV. Drake's [2], Yamamoto's [10] and Broder's [14] data differ significantly from the results of other authors. These results were given as low weighting when performing the spline approximation.

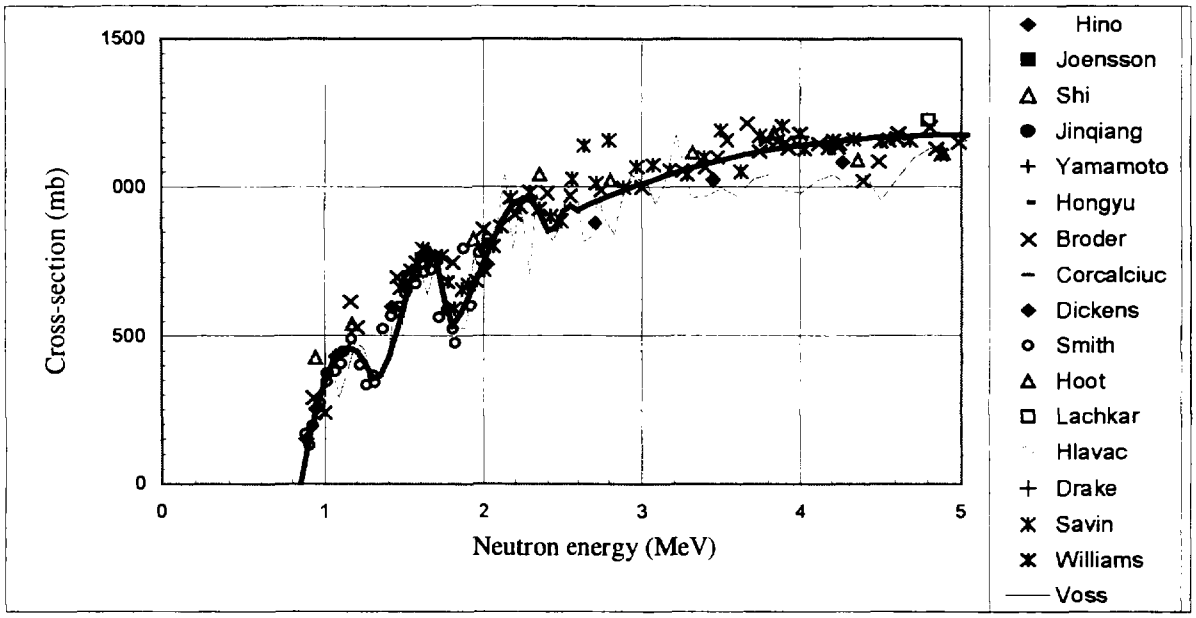

Fig. 4. Production cross-section for the E_γ = 846.8 keV gamma line (thick line - evaluation).

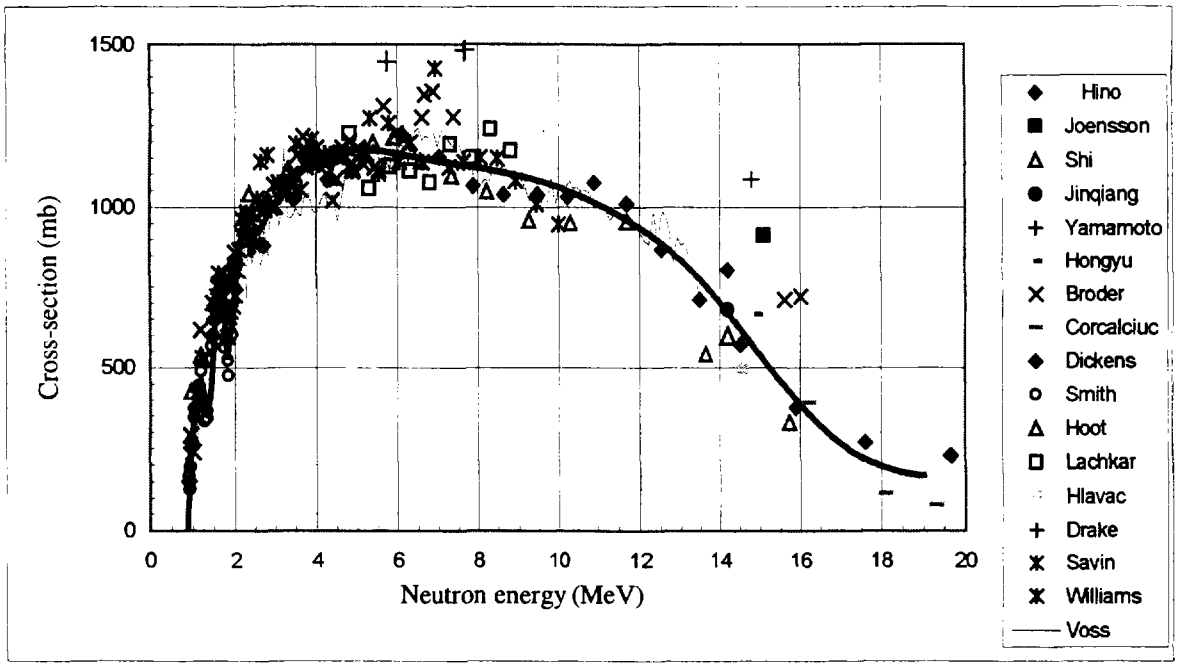

Fig. 5. Production cross-section for the E_γ = 846.8 keV gamma line (thick line - evaluation).

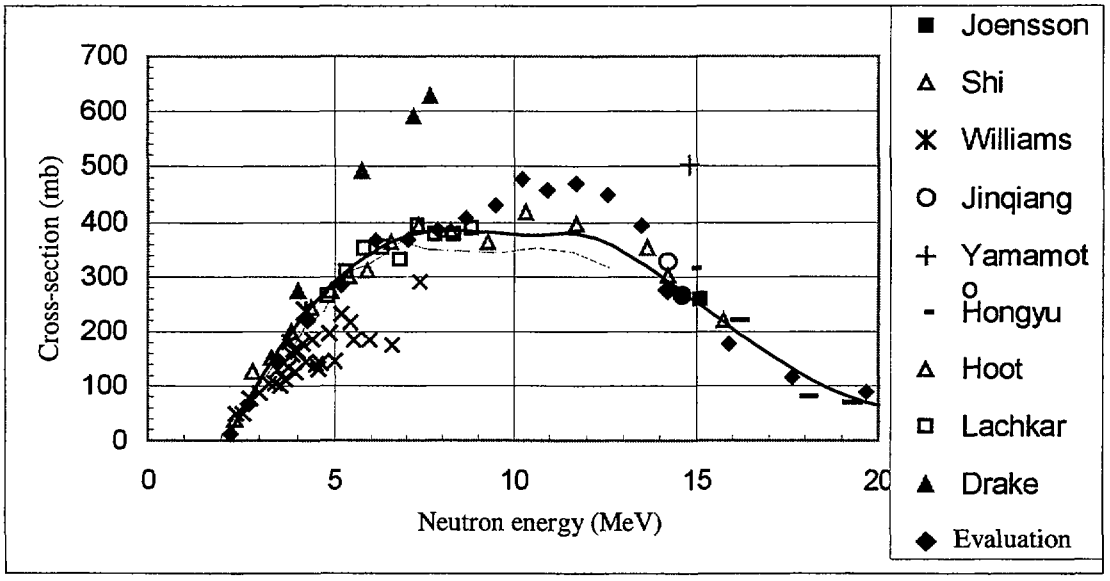

Fig. 6. Production cross-section for the E_γ = 1238.3 keV gamma line.

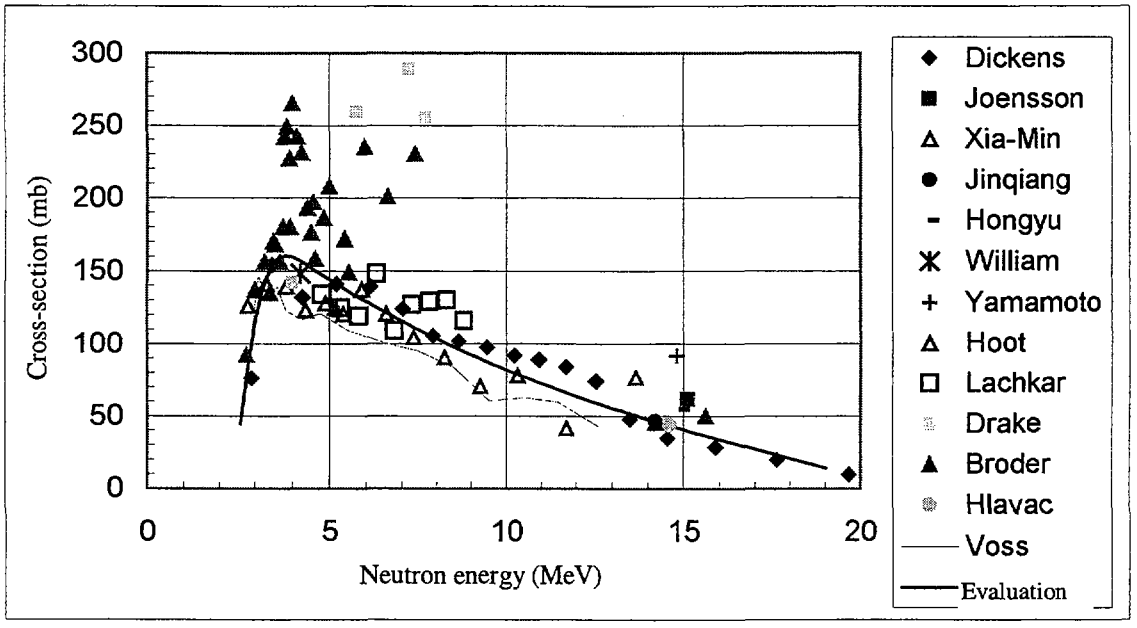

Fig. 7. Production cross-section for the E_γ = 1810.3 keV gamma line.

1810.8 keV line

The experimental results and the evaluated data for the 1810.8 keV gamma line are shown in Fig. 7. Voss's data in Ref. [22] are averaged over broad energy intervals - $\Delta E \cong 0.2$ MeV.

The figure shows that the results obtained for monoenergetic neutrons (Drake [2], Broder [14]) differ greatly from the cross-sections measured using the time-of-flight method and a continuous neutron spectrum (Hoot [19], Voss [22], Dickens [23]). At the same time, the results for a continuous spectrum show a not unsatisfactory level of agreement with Lachkar's data [3] and, in the E_n = 14-15 MeV interval, with the results in Refs [8, 11, 12, 14].

Conclusion

In conclusion, with regard to the discrete gamma line production cross-sections, the error of the evaluated 847.8 keV gamma line production cross-section is 5-10% over the whole energy range; for the 1238.3 keV gamma line, the error is generally 10-15%. With regard to the 1810.8 keV line there is a high level of uncertainty, owing to the spread of data; further experimental and theoretical research is needed here.

The angular distributions are most significant in the neutron energy region close to the excitation threshold of the production level. At high energies, there is averaging with respect to momenta when many transitions merge.

There is considerable divergence in the data obtained via measurements using (d,T) neutrons, which, it would seem, is due to error in the determination of the neutron flux onto the sample.

The evaluated values of the coefficients α_2 and α_4 and the gamma-ray production cross-sections are given in Tables 4-8. The data are given for iron of natural isotopic composition.

Table 4

Evaluated values of the coefficients α_2 and α_4 of the Legendre polynomials used to describe the angular distributions of the discrete gamma lines

E_γ = 846.8 keV			E_γ =1238.3 keV		E_γ = 1810.8 keV	
E_n (MeV)	α_2	α_4	E_n (MeV)	α_2	E_n (MeV)	α_2
0.95	0.510	-0.4333				
1	0.480	-0.3562				
1.2	0.380	-0.2134				
1.4	0.320	-0.1850				
1.6	0.280	-0.1534				
1.8	0.240	-0.1264				
2	0.220	-0.1035				
2.2	0.205	-0.0843				
2.4	0.195	-0.0683	2.4	0.358		
2.6	0.188	-0.0552	2.6	0.345		
2.8	0.184	-0.0445	2.8	0.334	2.8	0.506
3	0.178	-0.0359	3	0.322	3	0.377
3.2	0.170	-0.0291	3.2	0.307	3.2	0.316
3.4	0.169	-0.0238	3.4	0.300	3.4	0.278
3.6	0.164	-0.0198	3.6	0.292	3.6	0.246
3.8	0.162	-0.0167	3.8	0.281	3.8	0.220
4	0.160	-0.0144	4	0.276	4	0.200
4.2	0.158	-0.0128	4.2	0.265	4.2	0.184
4.4	0.155	-0.0115	4.4	0.260	4.4	0.172
4.6	0.152	-0.0106	4.6	0.254	4.6	0.164
4.8	0.150	-0.0099	4.8	0.250	4.8	0.158
5	0.147	-0.0093	5	0.246	5	0.154
5.2	0.145	-0.0088	5.2	0.241	5.2	0.151
5.4	0.141	-0.0084	5.4	0.237	5.4	0.149
5.6	0.138	-0.0081	5.6	0.233	5.6	0.147
5.8	0.136	-0.0079	5.8	0.230	5.8	0.145
6	0.132	-0.0077	6	0.228	6	0.143
6.2	0.131	-0.0076	6.2	0.223	6.2	0.140
6.4	0.130	-0.0076	6.4	0.219	6.4	0.138
6.6	0.128	-0.0077	6.6	0.216	6.6	0.136
6.8	0.126	-0.0078	6.8	0.214	6.8	0.134
7	0.124	-0.0081	7	0.212	7	0.132
7.2	0.122	-0.0084	7.2	0.212	7.2	0.130
7.4	0.121	-0.0088	7.4	0.209	7.4	0.129
7.6	0.120	-0.0092	7.6	0.205	7.6	0.127
7.8	0.118	-0.0098	7.8	0.201	7.8	0.125
8	0.115	-0.0104	8	0.200	8	0.123

E_γ = 846.8 keV			E_γ =1238.3 keV		E_γ = 1810.8 keV	
E_n (MeV)	α_2	α_4	E_n (MeV)	α_2	E_n (MeV)	α_2
8.2	0.113	-0.0111	8.2	0.198	8.2	0.121
8.4	0.111	-0.0118	8.4	0.196	8.4	0.119
8.6	0.108	-0.0127	8.6	0.196	8.6	0.118
8.8	0.107	-0.0135	8.8	0.191	8.8	0.116
9	0.106	-0.0144	9	0.191	9	0.114
9.2	0.105	-0.0154	9.2	0.190	9.2	0.113
9.4	0.104	-0.0164	9.4	0.189	9.4	0.111
9.6	0.104	-0.0175	9.6	0.187	9.6	0.110
9.8	0.103	-0.0186	9.8	0.186	9.8	0.108
10	0.102	-0.0197	10	0.185	10	0.107
10.5	0.100	-0.0225	10.5	0.182	10.5	0.103
11	0.096	-0.0254	11	0.179	11	0.100
11.5	0.093	-0.0281	11.5	0.177	11.5	0.098
12	0.090	-0.0305	12	0.175	12	0.096
12.5	0.087	-0.0325	12.5	0.172	12.5	0.094
13	0.085	-0.0339	13	0.170	13	0.093
13.5	0.083	-0.0344	13.5	0.167	13.5	0.092
14	0.080	-0.0339	14	0.164	14	0.091

Table 5

Production cross-sections for discrete gamma rays with an energy of E_γ = 846.8 keV

E_n (MeV)	Cross-section (mb)	E_n (MeV)	Cross-section (mb)	E_n (MeV)	Cross-section (mb)	E_n (MeV)	Cross-section (mb)
0.85	5.01	2.45	863.70	6.60	1148.22	13.00	834.90
0.90	144.85	2.50	917.55	6.80	1143.99	13.20	810.74
0.95	258.83	2.55	936.71	7.00	1139.89	13.40	785.17
1.00	347.08	2.60	924.00	7.20	1135.86	13.60	758.13
1.05	409.78	2.65	936.20	7.40	1131.85	13.80	729.62
1.10	447.07	2.70	948.02	7.60	1127.82	14.00	699.82
1.15	459.11	2.75	959.47	7.80	1123.72	14.20	668.98
1.20	446.05	2.80	970.55	8.00	1119.50	14.40	637.33
1.25	408.05	2.85	981.26	8.20	1115.11	14.60	605.13
1.30	356.49	2.90	991.62	8.40	1110.51	14.80	572.61
1.35	366.86	2.95	1001.62	8.60	1105.64	15.00	540.03
1.40	426.63	3.00	1011.28	8.80	1100.46	15.20	507.63
1.45	516.67	3.05	1020.59	9.00	1094.93	15.40	475.65
1.50	617.80	3.10	1029.57	9.20	1088.98	15.60	444.34
1.55	710.89	3.15	1038.21	9.40	1082.59	15.80	413.94
1.60	776.79	3.20	1046.53	9.60	1075.68	16.00	384.70
1.65	796.33	3.40	1076.67	9.80	1068.23	16.20	356.87
1.70	750.37	3.60	1102.03	10.00	1060.18	16.40	330.68
1.75	619.76	3.80	1122.97	10.20	1051.48	16.60	306.38
1.80	533.98	4.00	1139.84	10.40	1042.09	16.80	284.21
1.85	575.54	4.20	1152.99	10.60	1031.95	17.00	264.38
1.90	628.57	4.40	1162.78	10.80	1021.03	17.20	246.80
1.95	688.79	4.60	1169.55	11.00	1009.26	17.40	231.36
2.00	751.94	4.80	1173.65	11.20	996.61	17.60	217.90
2.05	813.73	5.00	1175.44	11.40	983.02	17.80	206.30
2.10	869.90	5.20	1175.26	11.60	968.45	18.00	196.43
2.15	916.17	5.40	1173.48	11.80	952.85	18.20	188.14
2.20	948.27	5.60	1170.43	12.00	936.17	18.40	181.30
2.25	961.93	5.80	1166.47	12.20	918.36	18.60	175.78
2.30	952.88	6.00	1161.95	12.40	899.38	18.80	171.45
2.35	916.83	6.20	1157.22	12.60	879.17	19.00	168.16
2.40	855.18	6.40	1152.61	12.80	857.70		

Table 6

Production cross-sections for discrete gamma rays with an energy of $E_\gamma = 1238.8$ keV

E_n (MeV)	Cross-section (mb)	E_n (MeV)	Cross-section (mb)	E_n (MeV)	Cross-section (mb)	E_n (MeV)	Cross-section (mb)
2.20	8.39	6.80	370.11	11.40	380.17	16.00	204.39
2.40	35.85	7.00	374.39	11.60	379.84	16.20	194.91
2.60	62.15	7.20	377.87	11.80	378.22	16.40	185.56
2.80	87.28	7.40	380.60	12.00	375.41	16.60	176.36
3.00	111.28	7.60	382.65	12.20	371.48	16.80	167.35
3.20	134.15	7.80	384.09	12.40	366.55	17.00	158.52
3.40	155.91	8.00	384.98	12.60	360.71	17.20	149.92
3.60	176.57	8.20	385.39	12.80	354.04	17.40	141.55
3.80	196.15	8.40	385.39	13.00	346.66	17.60	133.44
4.00	214.66	8.60	385.04	13.20	338.65	17.80	125.60
4.20	232.13	8.80	384.41	13.40	330.10	18.00	118.07
4.40	248.55	9.00	383.57	13.60	321.12	18.20	110.85
4.60	263.95	9.20	382.58	13.80	311.80	18.40	103.96
4.80	278.35	9.40	381.50	14.00	302.23	18.60	97.44
5.00	291.75	9.60	380.41	14.20	292.51	18.80	91.30
5.20	304.17	9.80	379.38	14.40	282.72	19.00	85.55
5.40	315.63	10.00	378.46	14.60	272.88	19.20	80.22
5.60	326.14	10.20	377.72	14.80	263.02	19.40	75.34
5.80	335.72	10.40	377.24	15.00	253.14	19.60	70.91
6.00	344.38	10.60	377.07	15.20	243.28	19.80	66.96
6.20	352.13	10.80	377.28	15.40	233.46	20.00	63.51
6.40	358.99	11.00	377.95	15.60	223.69		
6.60	364.98	11.20	379.13	15.80	213.99		

Table 7

Production cross-sections for discrete gamma rays with an energy of E_γ = 1810.8 keV

E_n (MeV)	Cross-section (mb)	E_n (MeV)	Cross-section (mb)	E_n (MeV)	Cross-section (mb)	E_n (MeV)	Cross-section (mb)
2.60	44.70	6.80	118.31	11.00	72.13	15.20	39.04
2.80	85.29	7.00	115.70	11.20	70.32	15.40	37.66
3.00	115.67	7.20	113.14	11.40	68.54	15.60	36.29
3.20	136.92	7.40	110.62	11.60	66.78	15.80	34.94
3.40	150.48	7.60	108.15	11.80	65.05	16.00	33.59
3.60	157.81	7.80	105.72	12.00	63.35	16.20	32.26
3.80	160.33	8.00	103.34	12.20	61.67	16.40	30.93
4.00	159.50	8.20	101.00	12.40	60.02	16.60	29.61
4.20	156.76	8.40	98.69	12.60	58.40	16.80	28.29
4.40	153.49	8.60	96.43	12.80	56.79	17.00	26.98
4.60	150.27	8.80	94.21	13.00	55.21	17.20	25.68
4.80	147.10	9.00	92.02	13.20	53.65	17.40	24.38
5.00	143.99	9.20	89.88	13.40	52.11	17.60	23.08
5.20	140.93	9.40	87.77	13.60	50.59	17.80	21.79
5.40	137.92	9.60	85.70	13.80	49.09	18.00	20.50
5.60	134.97	9.80	83.66	14.00	47.60	18.20	19.21
5.80	132.07	10.00	81.66	14.20	46.14	18.40	17.92
6.00	129.22	10.20	79.69	14.40	44.69	18.60	16.63
6.20	126.42	10.40	77.75	14.60	43.25	18.80	15.34
6.40	123.67	10.60	75.85	14.80	41.84	19.00	14.04
6.60	120.96	10.80	73.97	15.00	40.43		

Table 8

Spline approximation coefficients for discrete gamma line production cross-sections

amma ray energy E_γ (MeV)	Knot energy (MeV)	A_0 (mb)	A_1 (mb/MeV)	A_2 (mb/MeV^2)	A_3 (mb/MeV^3)	Error $\Delta\sigma_{n,x\gamma}$ (mb) at the knot
0.847	0.85	5.00673	3056.678	-5205.465	206.9289	0.5034176
	1.25853	399.0849	-1683.515	16889.24	-25536.03	61.98173
	1.77459	518.6271	517.0054	3582.455	-5697.28	69.99478
	2.38724	869.9078	-1508.664	29158.96	-106710.4	75.95874
	2.57013	916.5241	252.5369	-77.84503	7.311781	47.50709
	6.261371	1155.78	-23.27785	3.123605	-0.9995274	46.84921
	13.6167	755.8115	-139.5534	-18.93195	5.099319	32.27791
	16.8083	283.3481	-104.5702	29.893	-2.811044	19.6597
1.240	2.23	12.58569	139.3748	-14.78536	0.3077466	1.324959
	6.9268	372.9234	20.85369	-10.44909	1.382759	5.428989
	11.2322	379.3714	7.773093	-18.37684	1.986758	5.016663
	14.1677	294.0896	-48.75668	-0.8804508	0.4220889	4.267272
1.810	2.75	76.09608	190.5655	-136.6633	30.07322	4.349928
	4.272715	155.5753	-16.44436	0.7155358	-0.01707704	2.339919

References

[1] S.N. Abramovich, B.Ya. Guzhovskij, V.A. Zherebtsov, A.G. Zvenigorodskij, Reference Handbook, GKAEh (USSR State Committee on the Utilization of Atomic Energy), Moscow (1989) pp. 27-34.

[2] D.M. Drake, J.C. Hopkins, C.S. Young, H. Conde, J. Nucl. Sci. Eng. v.40 (1970) pp. 294-305, EXFOR-10025.

[3] J. Lachkar, J. Sigand, Y. Patin, G. Haonat, Nucl. Scie. Eng. v.55 (1974) p. 168-187.

[4] D. L. Smith, Report ANL - NDM - 20 -1976 - EXFOR-10613.

[5] R.W. Benjamin, P.S. Buchanan, J.L. Morgan, Nucl. Phys. v.79 (1966) p. 241.

[6] F.C. Engesser, W.E. Thompson, WASH-1124 (1968) p. 134.

[7] B.M. Dzyuba, L.M. Lazarev, I.N. Paramonova, M.V. Savin, Voprosy Atomnoj Nauki i Tekhniki, Seriya: Yadernye konstanty, N1 (1985), pp 72-76.

[8] B. Joensson, K. Nyberg, I Bergqvist, J. Arkiv for Fisik v.39 (1969) p. 295, EXFOR-20164.

[9] Y. Hino, T. Yamamoto, T. Saito, Y. Arai, S. Itagaki, K. Sugiyama, J. Nucl. Sci. Techn. v. 15(2) (1978) p. 85, EXFOR-20626.

[10] T. Yamamoto, Y. Hino, S. Itagaki, K. Sugiyama, J. Nucl. Sci. Techn. v. 15(11) (1978) p. 797, EXFOR-21304.

[11] Shi Xia-Min, Shen Rong-Lin, Xing Jin Qiang, Shen Rong-Lin, Ding Da-Zhao, Chinese J. of Nuclear Physics (in Chinese) v. 4(2) (1982) p. 120, EXFOR-30656.

[12] Zhou Hongyu, Tang Lin, Yan Yiming et al., IAEA Report INDC (CPR)-10 (1986), EXFOR-30904, Chinese J. of Nuclear Physics v. 10 (1988) p. 166.

[13] Xing Jinqiang, Cao Zhong, Wu Yongshun, Chen Qun, Chinese J. of Nucl. Phys. (in Chinese) v. 10(3) (1988) p. 282, EXFOR-32513.

[14] S. Hlavac, P. Oblozinsky, IAEA report INDC (CSR) - 5[GI, Vienna (1983), EXFOR-30801.

[15] D.L. Broder, A.F. Gamamit, A.I. Lashuk, I.P. Sadokhin, Nuclear Data for Reactors, IAEA, Vienna (1970), v. II, pp 295-300, Proceedings of the Second International Conf., Helsinki, 15-19 June (1970).

[16] J. Lachkar, J. Sigand, Y. Patin, G. Haonat, Nucl. Scie. Eng. v. 55 (1974) p.168-187.

[17] V. Korkal'chuk, G.A. Prokopets, B. Kholmkvist, Yadernaya Fizika v. 20 N6 (1979) pp 1096-1105, EXFOR-40306.

[18] D.L. Smith, Report ANL - NDM - 20 (1976), EXFOR-10613.

[19] C.G. Hoot, V.J. Orphan, J. John, R., GULF-RT-A-10743 (1971), EXFOR-10219.

[20] M.V. Savin, I.N. Paramonova,Yu.A. Khokhlov, Nejtronnaya Fizika, Part 1, pp 282-289, Naukova Dumka Kiev, 1972, Materialy Vsesoyuznogo Soveshchaniya Kiev, 24-28 May (1971).

[21] M.V. Savin, Yu.A. Khokhlov, I.N. Paramonova, et al., Yadernaya Fizika v. 23 (1976) N3, EXFOR-40346.

[22] F. Voss, S. Cierjacks, L. Kropp, Report KFK-1494, Karlsruhe (1971).

[23] J.K. Dickens, C.Y. Fu, D.M. Hetrick, D.C. Larson, J.H. Todd, Nuclear Data for Science and Technology, p. 307-309, Proceeding of an Jut. Conf., Jülich, Germany, 13-17 May (1991), Report - ORNL-TM-11671 (1990), EXFOR-13500.